ORIGINAL ARTICLE

Assessment of the compressive mechanical behavior of injection molded E-glass/polypropylene by mechanical testing and X-ray computed tomography

Antonios G. Stamopoulos[1] · Francesco Gazza[2] · Giuseppe Neirotti[3]

Abstract

Nowadays, thermoplastic composite materials are considered among the most promising ones as they are gaining the interest of many industrial sectors due to their eco-friendly features such as their recyclability and their low-cost demand while being produced in high volumes. Among the most concerning issues regarding the injection molded, short fiber-reinforced composites are the fiber distribution, the fiber orientation, and their effect on the overall mechanical performance. In the present work, the effect of the injection molding on the compressive properties is investigated experimentally. In this context, compressive mechanical tests have been conducted in a range between subzero and elevated temperatures using specimens oriented parallel and perpendicular to the injection direction. In addition, X-ray computed tomography is implemented for characterizing some crucial features such as the fiber volume fraction, in local and global scale, and the orientation of the fibers through the thickness and length of the material. The results revealed a different compressive mechanical behavior between the two specimen categories in all the testing temperatures. In addition, the results obtained by the nondestructive testing revealed a significant variation of the fiber content locally and a notable difference between distinct zones through the thickness.

Keywords Injection molding · Mechanical properties · X-ray CT

1 Introduction

The composite materials are considered as an appealing solution to the automotive industry over the past years as they can derive an optimal result from both the structural and the aesthetical point of view. The interest demonstrated from both novel hybrid vehicle constructors and traditional vehicle manufacturers is increasingly high as the objective is the weight reduction for decreasing the fuel and energy consumption and deliver sustainable and safer structures [1]. These two factors are important as the decrease of the

vehicle weight may contribute to a greener, more efficient, and safer outcome that, as a product, performs even better. Considering the above statement, the weight saving when implementing composites instead of traditional metallic materials such as steel, iron, or aluminum can potentially achieve the levels of 15–25% in the case of glass fiber polymer composites (GFRPs) and up to 40% while using carbon fiber polymer composites (CFRPs) [2].

Among the existing categories of composites, those consisting of a thermoplastic polymeric matrix reinforced with short fibers are an appealing solution, especially for the automotive industry due to many advantages they exhibit such as their ease of fabrication implementing methods such as extrusion compound and injection molding [3]. In fact, a great percentage of the plastic or reinforced plastic components fabricated worldwide are made using the injection molding process because of its relative simplicity, cost-effectiveness, and the absence of severe defects such as wrinkles, burn marks, and large voids [4]. Therefore, it is considered as a mass production fabrication process, capable of delivering high quantities of high-quality products.

✉ Antonios G. Stamopoulos
antonios.stamopoulos@univaq.it

1 Department of Industrial and Information Engineering and Economics (DIIIE), University of L'Aquila, Monteluco di Roio, 67100 L'Aquila, Italy

2 Materials Engineering, Methods and Tools Italy, Centro Ricerche Fiat S.c.p.A., 10135 Torino, Italy

3 Innovation Square Center, SIGIT S.p.A., 10137 Torino, Italy

It mainly consists of 4 stages, namely, the melting of the polymeric material, which most of the times is consequently mixed with a quantity of short fibers or nanoparticles [5], the clamping of the molds for creating the cavity, the injection of the melted compound of polymer and fibers, and the cooling down, which is most of the times the time-consuming part of the process. The output, as material, considering that is reinforced even partially with chopped fibers, is destined to replace the exclusively plastic parts of a vehicle giving them superior mechanical characteristics and, therefore, a better product quality [5].

There has been reported a significant number of works aiming to identify some of the process parameters' influence on the quality of the produced component, mainly implementing a comparative mechanical characterization. Already, starting from almost 30 years ago, there have been some studies [6] concluding that the short fibers, mixed with a melted thermoplastic, tend to have a preferred orientation while are being injected into a cavity. Therefore, this orientation may be affected by several parameters such as the fiber content and size, the flow rate, the inlet temperature, and the topology of the cavity. The synergy of all these factors produces a certain uncertainty about this orientation which is prevalent for the optimum mechanical behavior of the composite product, leading to the development of anisotropies [7, 8]. In fact, several static tests, mainly tensile, in various relative angles of the orientation of the polyamide 6/glass fiber specimens and the mold flow direction were conducted by De Monte et al. [9] concluding that the tensile strength and modulus are decreasing as the specimen tends to align to the axis perpendicular to the injection flow while the deformation at break increases, a fact which indicates a preferential orientation of the fibers. In the same study, the level of anisotropy of the material in terms of both strength and elastic moduli was addressed in 3 reference specimen thickness, concluding that its mechanical performance changes radically while the thickness increases. Similar observations about the dependence of the tensile properties of injection molded polyamide/short glass fiber composite material were observed by Wang et al. [10] in various strain rates. In addition, Mortazavian and Fatemi [11] adopted a similar approach for assessing the tensile behavior of polybutylene terephthalate and polyamide 6, reinforced with short glass fibers, in a temperature range between −40 and 130 °C with varying strain rates. The same materials were also present in another work of the same authors [12] in which an observation was made about the through-the-thickness preferential orientation of the fibers; there was observed the formation of a core shell referring to the midplane with a finite thickness in which the fibers tend to align perpendicular to the mold flow while, on the contrary, in the regions near the outer walls of the specimen the fibers tend to orient towards the mold flow. The same observation was also stated in the

works of Gupta and Wang [13] and Zainudin et al. [14]. The concept of the existence of various layers through-the-thickness with different fiber preferential orientations was adopted also by Bay and Tucker [15]. The same concept alongside with modified rule of mixture was present in the works of Patcharaphun and Menning [16] and Miles and Rostami [17] while the effect of a potential fiber alignment towards the injection flow direction on the shear properties was presented in [18] and a numerical approach/study for assessing the reinforcement characteristics can be found in [19]. The most interesting modification though is the addition of the parameters related to the characteristics of the reinforcing constituent such as the fiber critical length and distribution to the rule of mixtures. In addition, in the work of Miwa and Horiba [20], there have been presented series of experiments in different rates and temperatures for providing equations for gaining data and to provide formulas for predicting the tensile strength of both carbon and glass fiber-reinforced thermosets. In most of the abovementioned works, the existence of layers with preferential or even random orientation is explained by the interaction of the injected polymer with the walls of the dies that must fill and the temperature variations while being injected. Nevertheless, to the author's knowledge, the mechanical behavior of short fiber-reinforced polymers under compressive loads has been studied significantly less, mainly accompanied by tensile testing as seen in the work of Liu et al. [21].

In the present work, an experimental campaign is presented using an injected polypropylene reinforced with short glass fibers. This campaign aims towards the complete characterization of the material under compressive loads in various service/testing temperatures. The corresponding properties are addressed as well as the failure mode in each case, aiming to understand the potential influence of the fabrication method on them, related to the reinforcement characteristics. In addition to the mechanical characterization, X-ray computed tomography is implemented for assessing the characteristics of the fibers in terms of preferential orientation and local variation of the content. The results revealed a strong dependence of the compressive behavior to injection direction and thus to the fiber distribution and orientation inside the material while, by using a detailed nondestructive method, presented is a detailed analysis of the reinforcement characteristics through the length and thickness of the specimens.

2 Materials

As the scope is to assess the compressive mechanical behavior of short glass fiber/polypropylene material, mainly for automotive applications, the fabrication is conducted using fully industrialized equipment. To this end,

Table 1 The nominal physical and thermal properties of the polypropylene used in the present work

	Nominal value	Unit
Physical properties		
Melt flow rate (230 °C/5.0 kg)	5	gr/10 min
Melt volume flow rate (230 °C/5.0 kg)	5	cm^3/10 min
Density (23 °C)	1.15	gr/cm^3
Thermal properties		
Vicat softening temperature (B50 method)	140	°C
Deflection temperature under load		
0.45 MPa, unannealed	155	°C
1.80 MPa, unannealed	140	°C

Fig. 1 Schematic representation of the dies used alongside with the geometry of the injection gate and the composite plate considered in the present paper
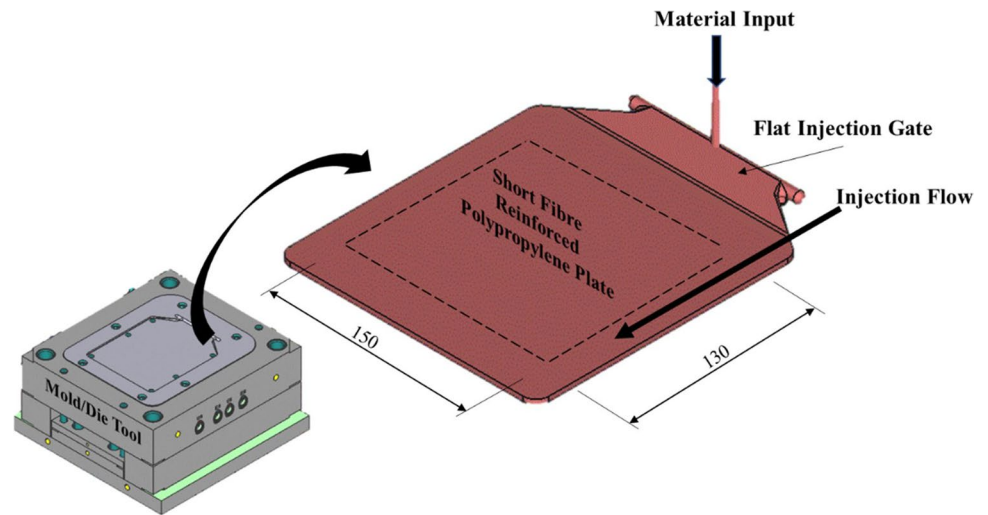
a commercial-grade polypropylene was selected that is UV-stabilized and mixed with 30% of weight fraction with short glass fibers. For the polypropylene, some specific data regarding its physical and thermal characteristics are reported in Table 1, as provided by the material supplier. On the other hand, regarding the short fibers that serve as the reinforcing agent of the composite material, their length follows a Gaussian distribution between 20 and 200 μm in order to comply with the internal standards of the Stellantis Group (Torino, Italy) for the specific application. For performing the injection molding, an Electron EVO 275 vertical injection molding machine is utilized (Centro Ricerche FIAT, Torino, Italy). A custom edge gate molding die (2-plate mold) with adjustable cross section is utilized that is typically used for producing large plates or thin-walled components [22, 23]. Instead of injecting directly the short fiber-reinforced polypropylene into the cavities with the form of compressive specimens that should be tested, an alternative strategy is put into practice: the material is injected inside a planar cavity and, after the cooling down process, plates of 200 mm length, 200 mm width, and of 4 mm of thickness are obtained. The cavity of the molds and the obtained plate is presented schematically in Fig. 1. The abovementioned

Table 2 The values of the basic parameters of the injection molding process for producing the short fiber GFRTP specimens

Parameter	Value	Unit
Screw diameter	50	mm
Dosage volume	240	cm^3
Dosage counterpressure	70	bar
Cylinder inner temperature	220	°C
Die inner temperature	35	°C
Speed	145	mm/s
Injection flow	80	cm^3/s
Injection volume	52	cm^3
Commutation volume	52	cm^3
Commutation pressure	364	bar
Holding pressure	350	bar
Holding time	20	s
Cycle time	62	s

strategy also justifies the use of edge gate molding dies. Regarding the injection molding process parameters, these are listed in Table 2. These parameters are properly selected based on previous experience in the field of the production

of planar components and plates with fiber dispersion as uniform as possible in the central part. In addition, for excluding any potential interaction between the walls of the dies and the reinforced polymer that can affect the output of the injection process, only the central part of the produced plate is considered for testing, as seen in Fig. 1. Therefore, from a plate 200 mm long and 200 mm wide, a smaller one of 130 mm length and 150 mm width is extracted.

3 Experimental

3.1 Mechanical testing

The mechanical testing campaign is about compressive tests in a varying service temperatures, from −30 up to 80 °C. These temperatures were carefully selected as they refer to the lowest, highest, and normal in-service temperature that

components of this material are designed for. As seen in the overall test matrix presented in Table 3, the injection direction is considered, labeling the specimens as InFlow, having their length oriented towards the injection direction, and CrossFlow, length oriented perpendicularly as seen in Fig. 2a.

The compressive specimens are fabricated and tested using the ASTM D695 standard [24]. From all the types of specimens suggested by this testing standard, in the present work, the prismatic shaped one is considered, and the topology of it is depicted in Fig. 2b. As previously mentioned, the specimens are not directly injected into shape, but extracted from the center of the plate described in Section 2 of the present work using a high-precision CNC milling machine equipped with an appropriate tool for mild plastics and composite materials. The corresponding rotational speed applied is relatively low, according to the ISO 2818 standard [25]. This way, not only the accuracy and repetitiveness of the

Table 3 The test matrix of both the compressive testing and the X-ray CT scanning campaign

Testing temperature (°C)	Testing speed (mm/min)	Specimen orientation	Specimen label	X-ray CT scan
−30	1	InFlow	Sp.1-30	
			Sp.2-30	
			Sp.3-30	
			Sp.4-30	
			Sp.5-30	
		CrossFlow	Sp.1-30	
			Sp.2-30	
			Sp.3-30	
			Sp.4-30	
			Sp.5-30	
25		InFlow	Sp.1-25	☒
			Sp.2-25	
			Sp.3-25	
			Sp.4-25	
			Sp.5-25	
		CrossFlow	Sp.1-25	☒
			Sp.2-25	
			Sp.3-25	
			Sp.4-25	
			Sp.5-25	
80		InFlow	Sp.1-80	
			Sp.2-80	☒
			Sp.3-80	
			Sp.4-80	☒
			Sp.5-80	
		CrossFlow	Sp.1-80	
			Sp.2-80	
			Sp.3-80	☒
			Sp.4-80	☒
			Sp.5-80	
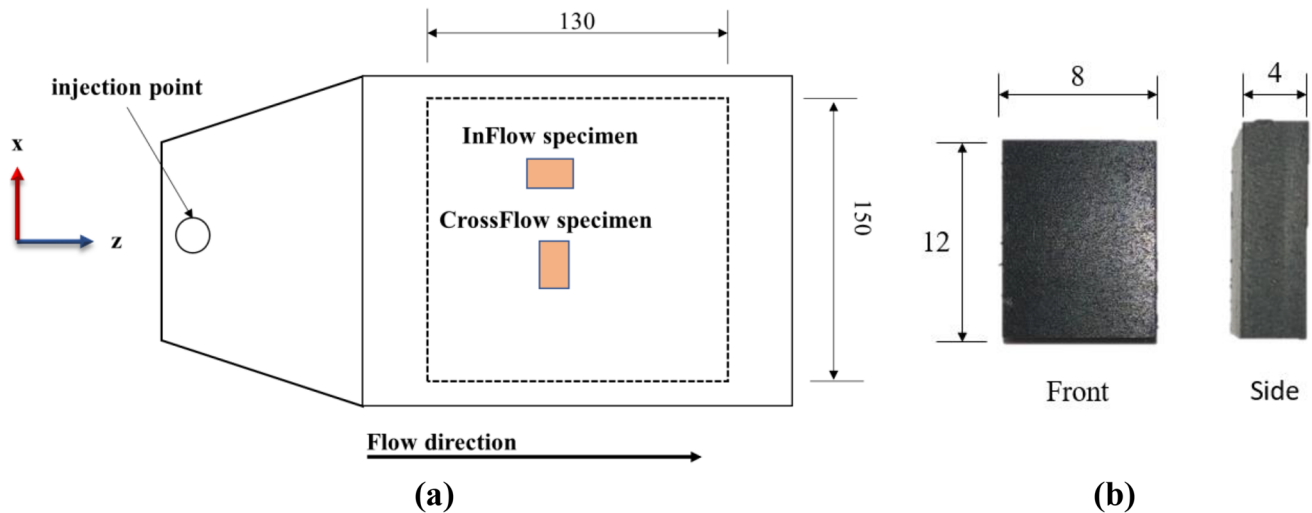
Fig. 2 Plate dimensions and orientation of the InFlow and CrossFlow specimen (**a**) and the basic geometry of the compression test specimen (**b**)

dimensions and tolerances imposed by the standards are fulfilled, but the smooth surface roughness is guaranteed as well as the absence of visual cracks and defects, also respecting the roughness ISO grade number that must be less than 8 for such small gage sections.

For the execution of the experimental campaign, an MTS Criterion 43.50 servo-electrical universal testing machine of 50 kN load capacity equipped with an MTS ThermaKraft climatic chamber with capacity from −150 to +300 °C is implemented. The machine crosshead speed is 1 mm/min which corresponds to the lowest static load as described by the corresponding testing standard. For achieving the subzero temperature of −30 °C while testing, nitrogen gas is infused in the climatic chamber. The infusion is automatically controlled by the corresponding testing machine controller for maintaining the temperature conditions stable. For ensuring the temperature uniformity of the specimens, a mild conditioning is conducted before the execution of the tests by introducing the required testing temperature for at least 30 minutes before the execution of each test. Moreover, considering the thermal expansion of the material at higher-than-ambient temperatures and the fact that stresses may be introduced, the upper part of the specimens remains free of pressure from the MTS testing plates during the whole execution of the sample conditioning. This way, any undesired deformation and preload are avoided. Finally, regarding the strain field measurement, a 2D Digital Image Correlation system is utilized, similar to the one presented in previous works in the field [26]. To this end, an appropriate pigmented pattern was previously introduced using a temperature-resistant acrylic-based color. For the calculation of the strain field, a reference image is selected at the start of the testing procedure and compared with the next frames using the MATLAB's Ncorr algorithm [27]. The procedure

alongside with the specimen during testing is presented in Fig. 3.

3.2 X-ray computed tomography

Among the existing NDT methods, the X-ray computed tomography appears to be the most promising for conducting 3D analysis and visualization of the microstructure of composite materials as seen in an important number of previous works [28, 29]. For instance, in the work of Baran et al. [30], this method was used for quantifying the fiber misalignment while defects in terms of porosity have been quantified in the works of Stamopoulos et al. [31] or Tserpes et al. [32] where XCT has also been used for the development of predictive models. More recently, some works have been presented also in the field of quantification of some characteristics of the internal structure of short-fiber composites such as the one of Chen et al. [33] in which fiber alignment was quantified in samples fabricated using selective laser sintering. In addition, regarding the injection molding process, the applicability of computed tomography for measuring the fiber direction was investigated by Hannesschläger et al. [34]. In all cases, the X-ray CT provided the advantages of the in-depth detection of crucial defects, the quantification of their characteristics, and their 3D visualization.

In the present work, the X-ray computed tomography is implemented in mainly 2 directions, namely, the identification of the distribution of the fibers and the corresponding content locally and the identification of the failure mechanism. To this end, 1 specimen from each category of injection flow direction for the case of the ambient temperature and 4 for the case of elevated temperatures (2 for each of the specimen orientation), as reported in Table 3, are scanned utilizing a GE phoenix v|tome|x s X-ray CT scanner
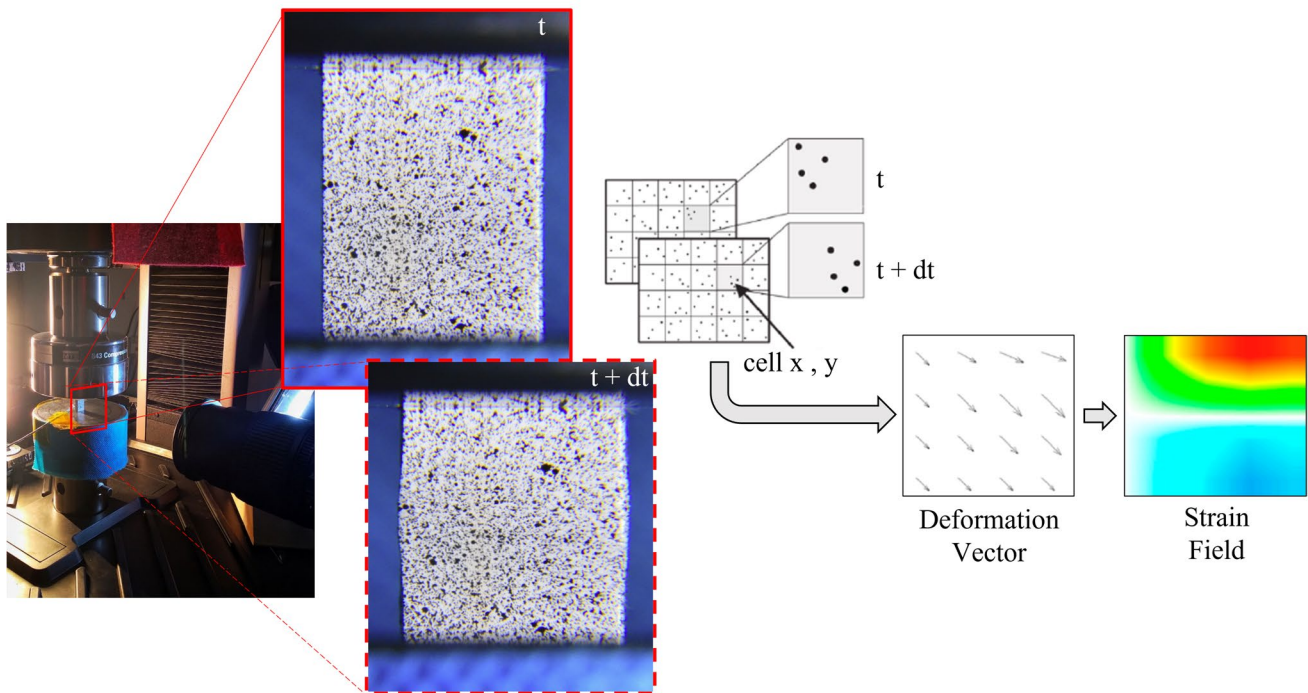
Fig. 3 Photos taken during the compressive testing of PP/short GF specimen in different instants with schematic explanation of the DIC procedure

equipped with high-power focus tubes in the premises of the ISC laboratory (SIGIT S.p.A., Turin, Italy). Considering the scanning parameters, the tube voltage was adjusted to 70 kV, the current at 90 µA, and 2000 projections of each of the samples were acquired while the voxel size was 12 µm. The 3D image reconstruction and analysis are performed using the VG Studio MAX 3.5 software [32, 34] CT reconstruction and the fiber composite material analysis module, respectively. Thresholds are imposed using the example areas and calculated automatically by the software's modules. For distinguishing the object from the background, the automatic ISO50 threshold is imposed.

For the determination of the fiber content and orientation, an analysis is conducted by creating a region of interest (ROI) in each of the samples that excludes the highly deformed external edges, as seen in Fig. 4. Consecutively, an integration mesh consisting of cubic cells of roughly 0.38 mm each is imposed, a value automatically generated by the software for segmenting the ROI. This mesh is oriented in a way that the cubic cell's orientation system (local) corresponds to the global Cartesian coordination system of the samples as seen in Fig. 4. Furthermore, after the abovementioned analysis, the distribution of the volume fraction is obtained in terms of a graph containing the number of cells and the corresponding fiber volume fraction (vf %) as well as the tensors of the fiber direction. This way, the two critical parameters, namely, the local and global fiber content and

the fiber orientation, may be identified. The procedure is applied in all of the specimens, with preferential direction of the length either Inflow or CrossFlow, creating a rectangular ROI dimensioned 10 mm long (direction z), 8 mm wide (direction x), and 3.6 mm thick (direction y).

4 Results and discussion

### 4.1 Compressive behavior and failure characteristics

The compressive mechanical behavior in terms of stress-strain curves for the 3 testing temperatures and 2 orientations, InFlow and CrossFlow, respectively, is reported in Fig. 5. As observed, the specimens oriented towards the injection direction (InFlow) demonstrate slightly higher values of strength while the difference between them is more intense at 80 °C. The corresponding properties in terms of average values of strength, compressive moduli, and deformation at brake are also reported in Table 4.

As seen in both the stress-strain curves and the corresponding mechanical properties, the testing/service temperature has a detrimental effect on both the elastic moduli and strength, attributed to the alteration of the properties of the polymer that are susceptible to the temperature conditions. For instance, in normal temperature, the material exhibits
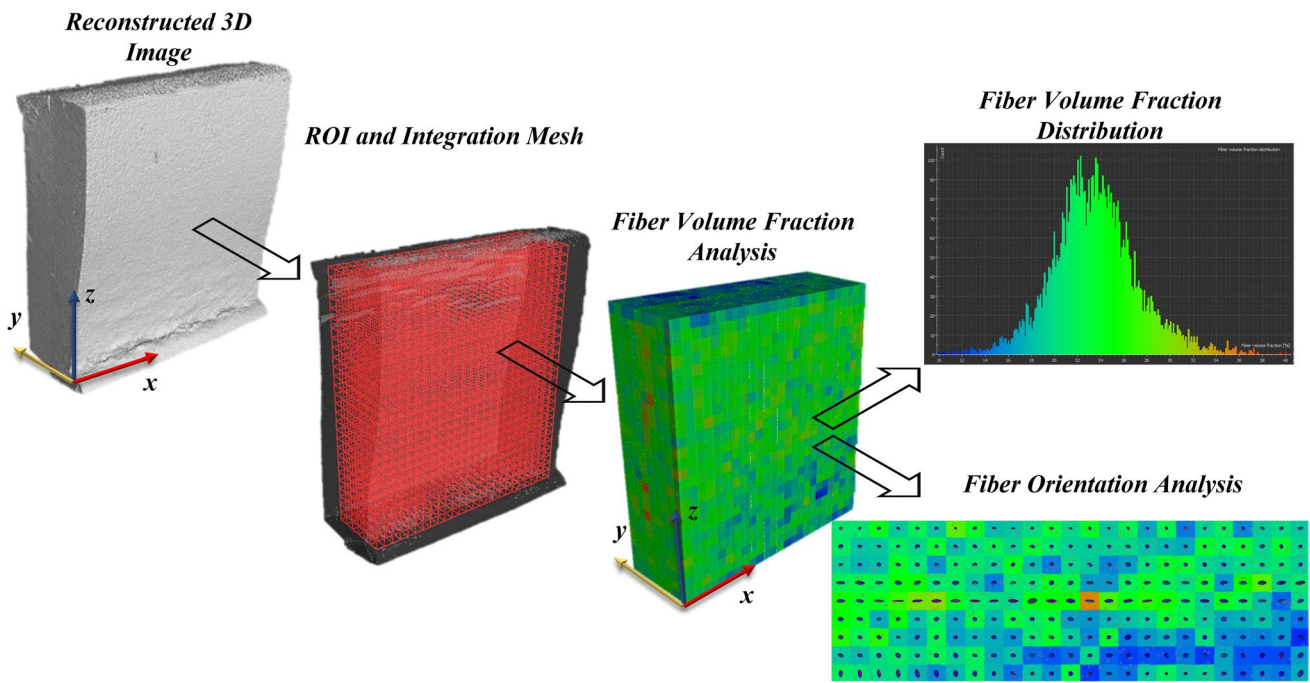
Fig. 4 Analysis of the determination of the region of interest (ROI), the integration mesh, and the characteristics of the fiber volume fraction and orientation analysis

Fig. 5 Compressive stress-strain curves of the InFlow and CrossFlow specimens in the 3 temperatures of interest
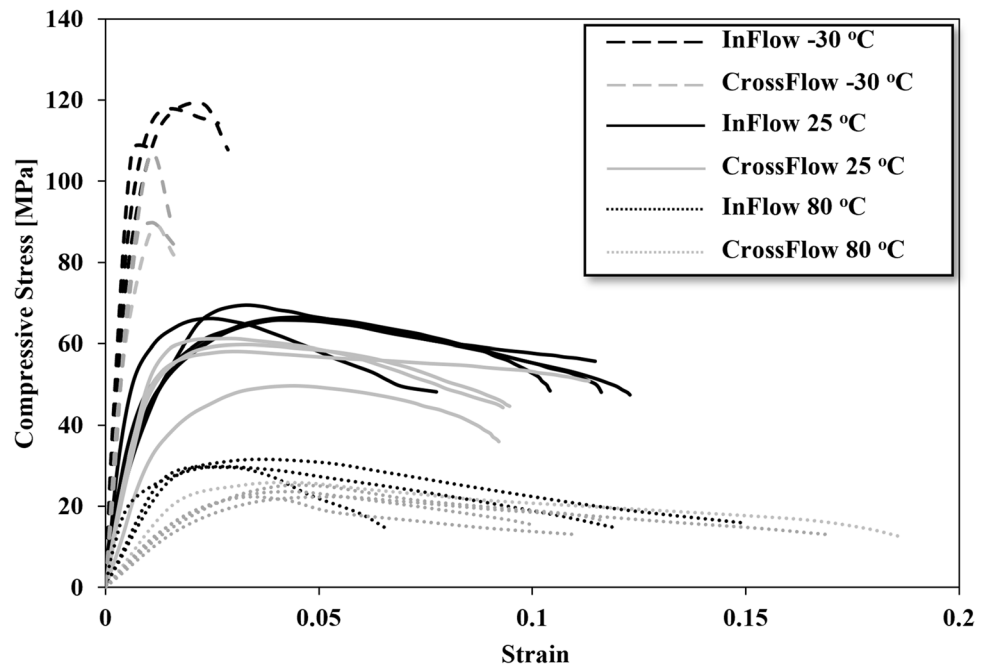
a compressive strength between 57.2 and 66.91 MPa and a maximum strain of roughly 10%. The strength is almost doubled while moving to subzero temperatures, with a significant decrease of the strain at break, and almost half when the temperature is elevated to 80 °C. A very interesting aspect is the difference between the In and CrossFlow specimens in

various temperatures. For instance, in the work of Patcharaphun and Menning [16], it is stated that the tensile strength S_u of a short fiber composite material may be predicted by a modified rule of mixtures where the component related to the fibers is multiplied by 2 factors, namely, the fiber orientation efficiency factor f_0 and the one related to the fiber

Table 4 The average values of the compressive mechanical properties of the InFlow and CrossFlow specimens at the 3 testing temperatures

Specimen type	Testing temperature (°C)	Compressive modulus (GPa)	Standard deviation (GPa)	Compressive strength (MPa)	Standard deviation (MPa)	Strain at break (%)	Standard deviation
InFlow	−30	16.67	0.20	112.44	4.46	2.23	0.61
CrossFlow		13.50	0.17	101.22	3.12	1.63	0.08
InFlow	25	7.77	0.06	66.91	1.48	10.71	1.01
CrossFlow		4.84	0.08	57.20	3.18	9.83	0.82
InFlow	80	2.25	0.75	31.20	2.09	12.08	1.89
CrossFlow		0.82	0.04	23.90	1.61	13.62	2.39
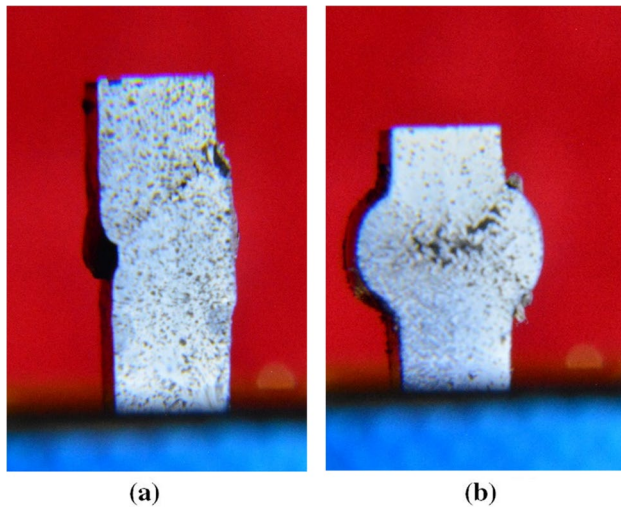
Fig. 6 The two typical failure modes observed in the compressive testing experimental campaign

critical length f_l. In particular, regarding the first one, it is also defined experimentally in the work of Miles and Rostami [17] in values between 1 for the case of a complete fiber alignment towards the load axis (perfectly unidirectional) and 0.2 in the case of a complete arbitrary fiber orientation. Therefore, the fibers' orientation is important for the maximization of their contribution to increase the mechanical properties of the composite material. In the case of the present study, the results reported by the compressive tests indicate superior mechanical compressive properties for the case of the InFlow specimens where the fibers appear to be more parallel to the loading axis compared to the CrossFlow ones. Nevertheless, taking into consideration the standard deviation of the results, the difference between the two specimen categories also indicates that the fiber alignment is significantly far from the perfect alignment towards one direction in either case.

Regarding the failure mode of the specimens, typically 2 types are observed and listed in Fig. 6 where a typical In (a) and a CrossFlow (b) specimen are presented. The first one is more frequently observed and is characterized by the formation of a diagonally oriented knee, seen in Fig.6a, that indicates a shear failure and is often observed in composite structures, while subjected to compressive loads. The second one, seen in Fig.6b, is less frequent and is about the formation of a barrel-type failure accompanied by diagonal cracks and the development of a void at the center of the specimen. This particular type is observed in a limited number of CrossFlow specimens. By analyzing the X-ray CT data, some observations about the failed samples can be obtained. In Fig. 7, a 3D isometric transparent view of the specimens of Fig. 6 is presented for addressing the characteristics of the failed specimens. In addition to this, the side view of both cases is presented for providing a spherical understanding of the failure mode. In both cases, the failure zone is indicated inside the red frame. Starting from the most common one, the shear failure, there can be observed a misalignment of the fibers inside the zone that is caused by the shearing of the specimen, making this region of the specimen particularly different from the rest of it. On the contrary, the specimen that demonstrated the failure mode seen in Fig. 7b has a slightly different failure mode composed by 2 zones that are buckled in the opposite direction regarding the y-axis, creating a crack/void between them. This failure mode is, presumably, the result of the nonuniform material properties locally that is caused by the irregular fiber distribution and orientation. In these particular cases, there has been observed, in some zones near the voids, a fiber content significantly lower compared to the average one, as seen in Section 4.2 of the present work. In addition, also considering the fact that this particular failure mode was observed mostly in high-temperature tests, there cannot be excluded the influence of some phenomena related to creep. It should be noted that the majority of the specimens fail under the shear-like failure mode seen in Fig. 7a, especially in normal and lower temperatures where the fracture was more brittle. On the contrary, the failure mode seen in Fig. 7b is far less frequent as it was obtained by only 3 specimens.

Fig. 7 Transparent 3D and side view of the InFlow (**a**) and CrossFlow (**b**) specimens with the corresponding failure zones as seen in the VG Studio MAX software


(a)   (b)
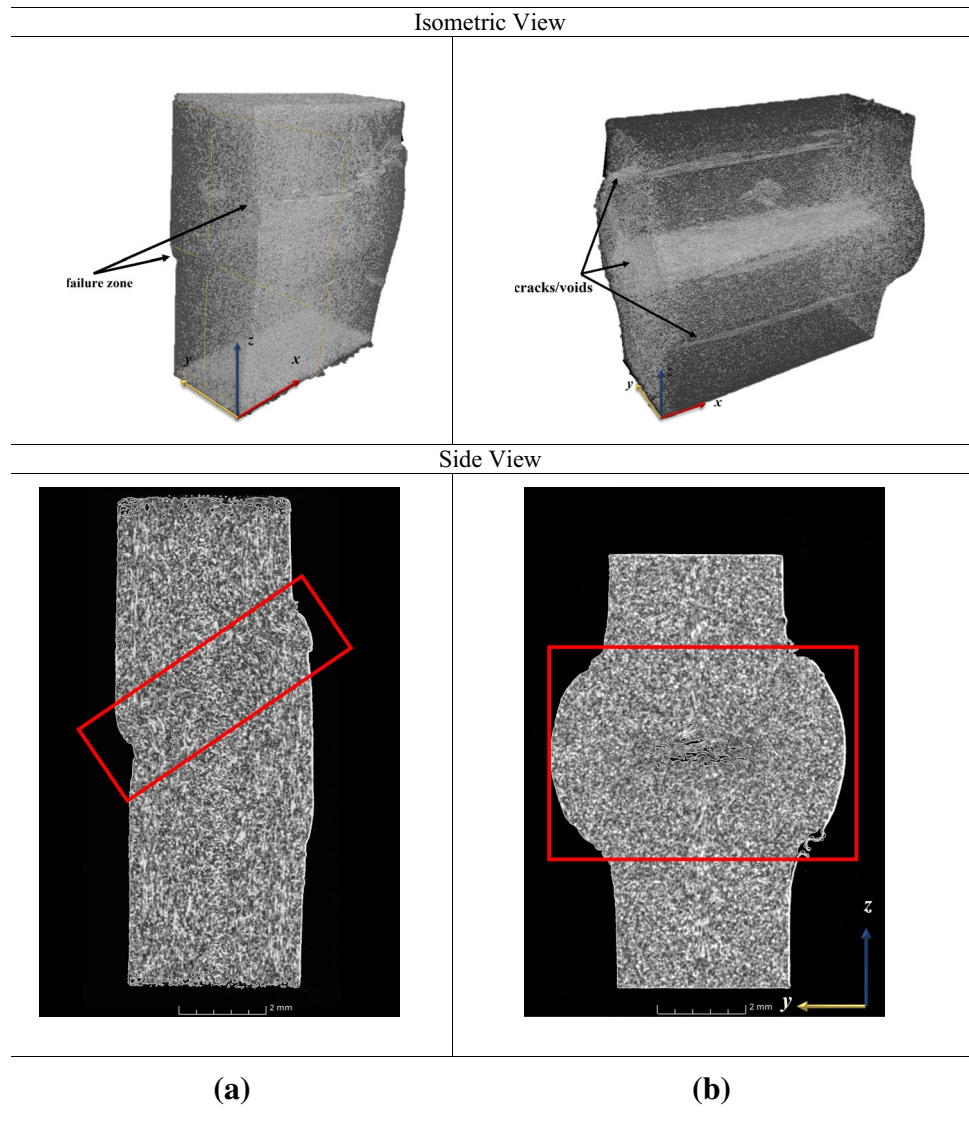
4.2 Quantification of fiber characteristics

As previously explained, the two most important characteristics are considering the homogeneity of the distribution of the fibers inside the specimens (fiber vf) and the preferential orientation of them with respect to the injection direction (fiber orientation).

4.2.1 Fiber content and distribution

Starting with the first parameter, in Fig. 8 is presented the number of cells of the integration mesh with the corresponding fiber content as measured by the image analysis module of the software presented in Section 3.1, where the cells colored blue have lower values of fiber volume fraction while the red the highest. The specimens tested at ambient temperature are distinguished from those tested in elevated

ones. In all of the cases, the cells' fiber volume fraction appears to be distributed quite normally with peak values around 30%. However, also considering the fact that all these specimens were cut from the same plate, there can be noted some significant differences between them regarding the distribution of the volume fraction assigned in the segmentation cells. For instance, the InFlow specimen used for testing at 25 °C appears to have significantly higher number of cells with fiber content around 30% while the Crossflow specimen less at 30% but significantly more with higher fiber content. Therefore, there are differences between them in terms of homogeneity of their fiber content as the InFlow has more cells concentrated in the zone between 25 and 40% while the CrossFlow presents lower concentration (number of cells) but in higher values (between 27 and 45%). The same observations can also be made for the specimens utilized for testing at 80 °C where the InFlow Sp.4 derives a higher number
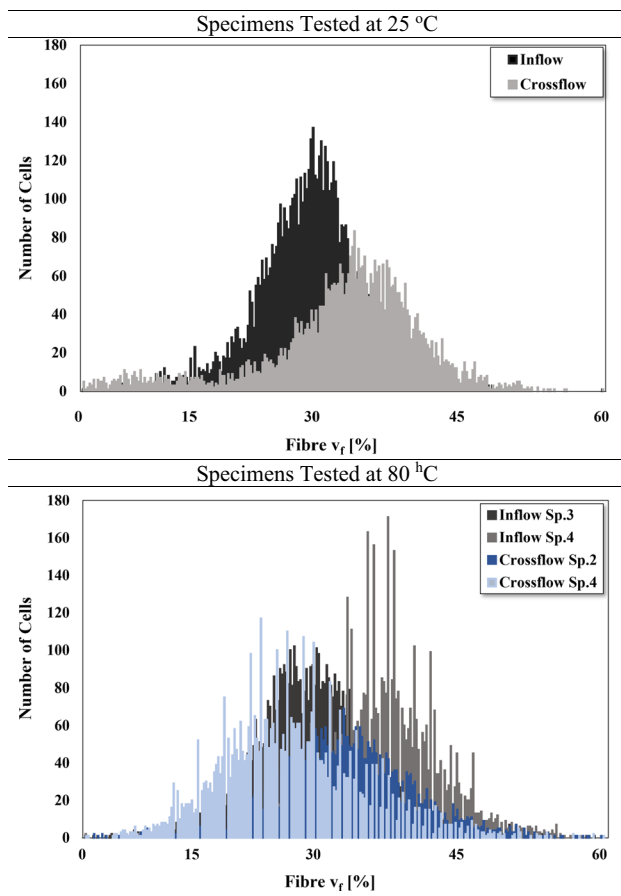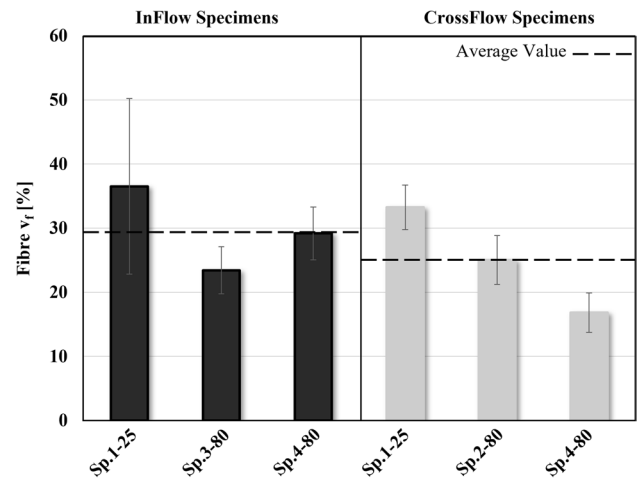
Fig. 8 Distribution of the fiber v_f in the cells of the integration mesh of both the InFlow and CrossFlow specimens

Fig. 9 The average fiber volume fraction (v_f) of all the specimens measured by XCT data analysis

of cells between 35 and 47% which differs it from the rest of the specimen, especially from the CrossFlow Sp.4 that demonstrates lower population of cells compared to the InFlow Sp.4 but also concentrated in values between 12 and 35%.

In terms of specimen fiber volume fraction, the results represent the average value of the fiber content of the cells in which the specimen was segmented into. The results accompanied by the corresponding standard deviation are presented in Fig. 9. There can be observed a difference between the specimens; for example, the Sp.1-25 InFlow specimen appears to have the highest average volume fraction while the Sp.4-80 CrossFlow the lowest. The average volume fraction of the InFlow specimens was slightly higher than the CrossFlow ones (29.7% compared to 25%) while, since they are all part of the same plate, the overall average fiber volume fraction is 27.37%.

4.2.2 Analysis of the fiber orientation

Given the fact that the preferential fiber orientation is a crucial, yet difficult to investigate, factor that according to the

literature has a detrimental effect on the mechanical properties of short-fiber composites, each of the cells of the integration grid/mesh obtained by the XCT image analysis can derive the averaged individual preferential direction of the fibers that are included inside it. In the work of Baradi et al. [35], the through-the-thickness distribution of the fiber orientation inside the weld line of injection molded composites was investigated and segmented into 4 zones, namely, the skin that corresponds to a thin region near the outer surface of the specimen that interacts with the molds, the shell that is a wide region between the skin and the midplane, an intermediate zone before the central part, and the core. The same approach is adopted in the present work, and the specimen is segmented accordingly to these zones as seen in Fig. 10 for the case of a CrossFlow specimen.

The VG Studio MAX fiber analysis module regarding the preferential direction can derive a schematic representation of the preferential direction of the fibers of each of the cells, given by a circular disc as seen in Figs. 10 and 11, respectively. In the present analysis, for excluding the zones highly affected by the molds during the injection process, the zones are segmented into the core zone where the fibers appear to be aligned perpendicularly to the injection direction and the intermediate zone where the orientation is more uniform, and the fibers are aligned parallel to the flow. This pattern seems to be repeatable for all of the samples and remains almost constant while moving through the x-axis. For having a better understanding of the through-the-thickness orientation of the fibers, a region of cells of a part of the specimens not affected by the compressive testing is considered. Consecutively, the central part of the width cells is taken into consideration and the relative fiber orientation tensors are obtained as seen in Fig. 11 where the case of an InFlow-oriented specimen is presented. As seen in the same figure,
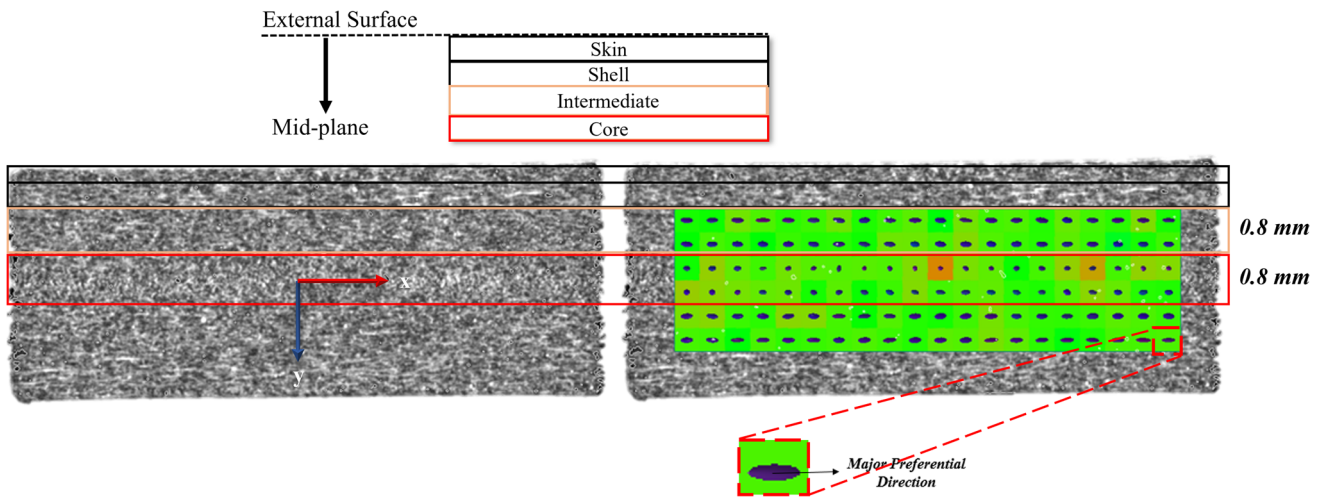
Fig. 10 Through-the-thickness segmentation of the specimen in zones in the base of the fiber orientation tensors

Fig. 11 Analysis of the fiber orientation tensor for various positions through-the-thickness of the central part of the undamaged zone of an InFlow specimen
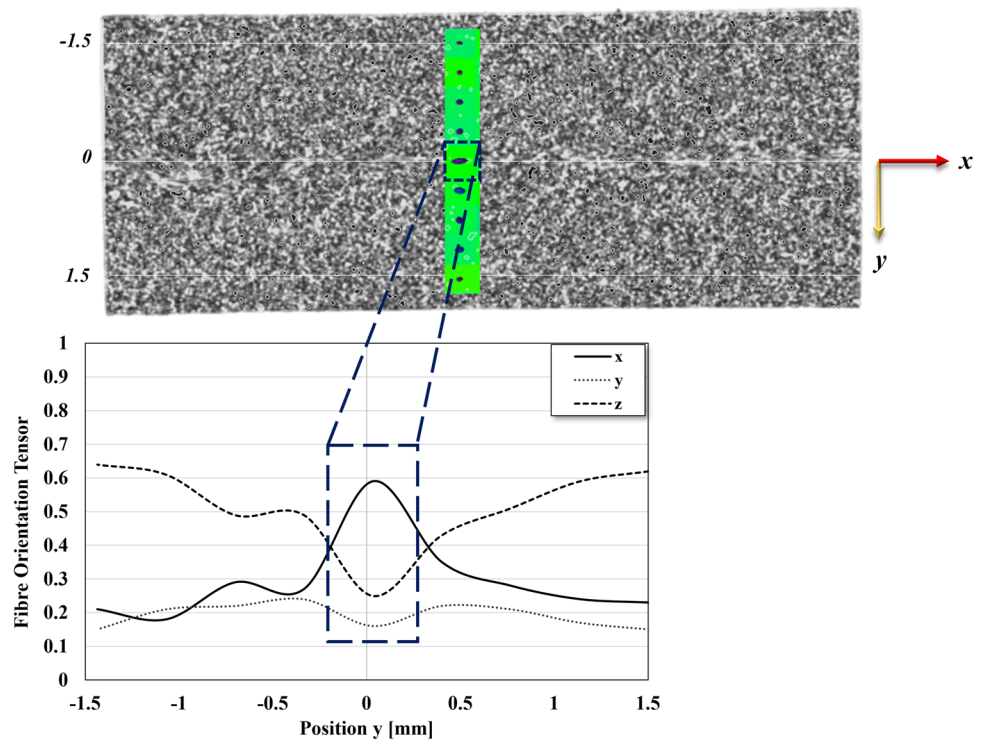
the midplane region of approximately 0.4 mm presents high values of the x tensor (towards the width, perpendicular to the injection direction). This changes while moving away from the midplane and the fibers are oriented prevalently towards the z-axis (parallel to the injection), deriving a fiber orientation tensor up to 0.68 while the orientation tensor towards the x direction drops down to 0.2.

A comparison between the In and CrossFlow samples regarding the through-the-thickness fiber orientation is presented in Fig. 12. It should be noted that, in all the cases,

the prevalent orientation tensor does not exceed the value of 0.7 which means that the fibers are not aligned perfectly to one of the main global axes x, y, or z of the specimen. There can be observed a certain pattern of the fiber orientation tensors of the InFlow samples, similar to the one described in Fig. 11. Regarding the CrossFlow samples, the core region's prevalent fiber tensor is the one towards the length of the specimen (direction towards the z-axis), parallel to the injection direction while the fibers away from the core zone are oriented perpendicularly to the material flow
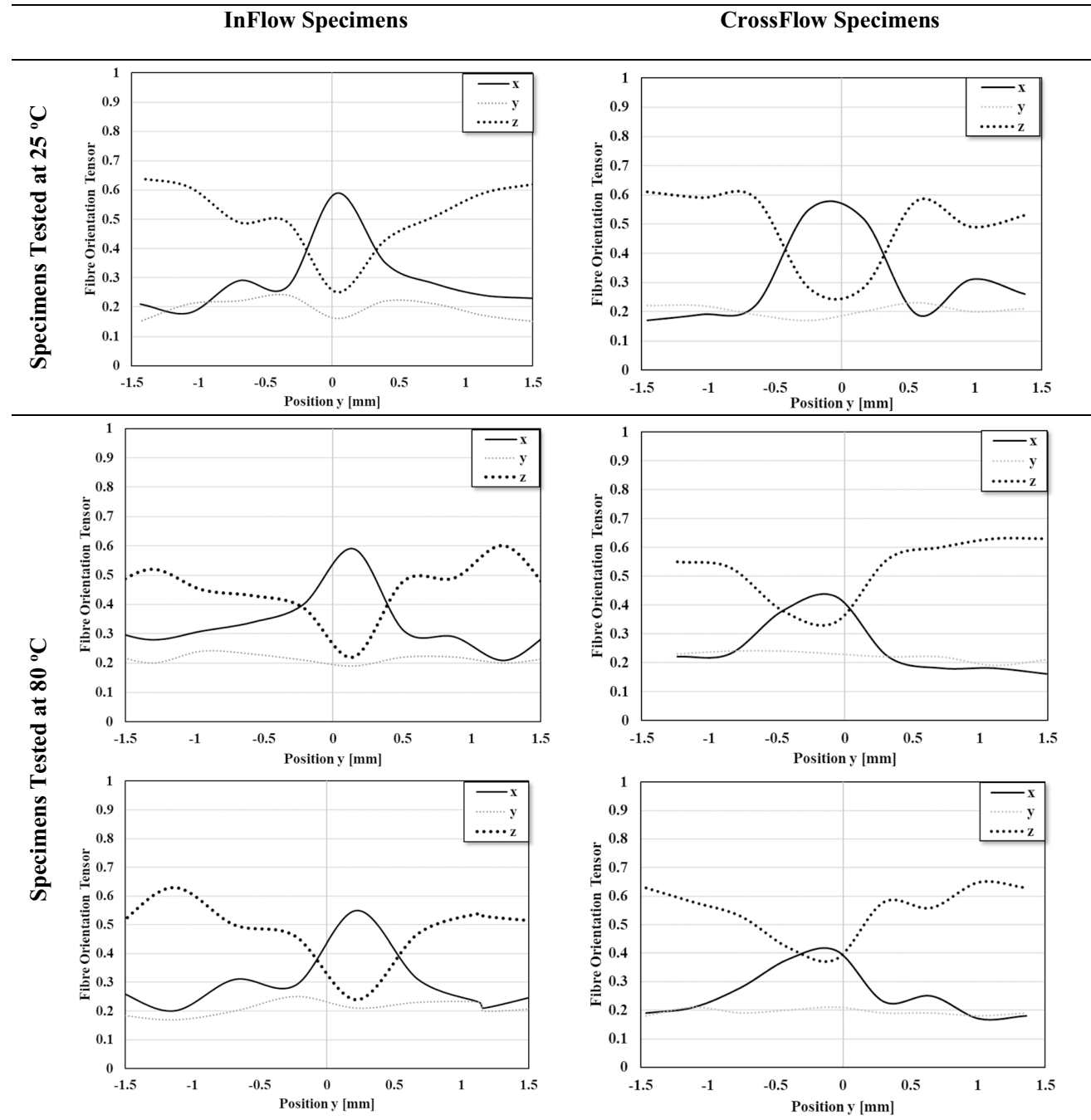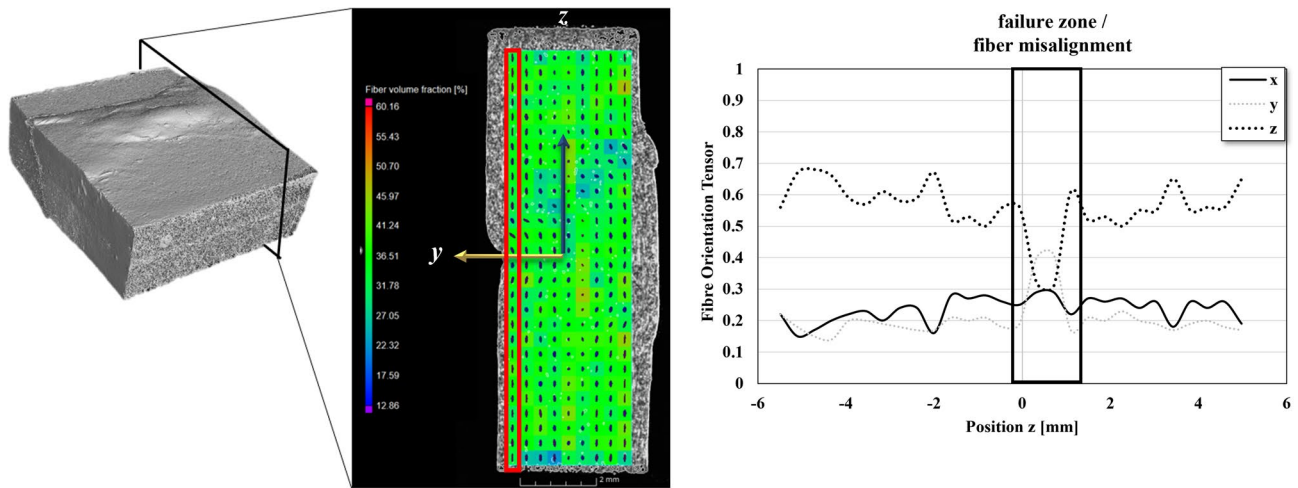
InFlow Specimens   **CrossFlow Specimens**

Fig. 12 The through-the-thickness fiber orientation tensors of the InFlow and CrossFlow specimens

direction (direction towards the *x*-axis). This fact can explain the failure mode observed in Section 4.1 of the present work where failure is located predominantly at the central part of the specimens in which the fibers' preferential direction is perpendicular to the applied load. All the results and observations are consistent with the ones observed in the works of Baradi et al. [35] or Fiebig and Shoeppner [36] where the fiber orientation factor is assessed.

Finally, regarding the through-the-length orientation of the fibers, it was found to be constant for a given position through the width and thickness of each of the specimen, away from the external surface and the thickness midplane, with a notable variation at the failure zones. In Fig. 13, a typical fiber orientation tensor distribution for the case of the InFlow Sp.1-25 specimen is presented for a zone away from the central one (core). The larger portion of fibers is

Fig. 13 The through-the-length fiber orientation tensors for the case of the InFlow Sp.1-15 specimen

oriented mainly towards the z-axis (length) that corresponds to the injection flow direction, achieving values up to 0.7. There can also be noted a fiber misalignment caused by the compression of the specimen that creates the failure zone where the z-tensor drops to 0.31. The results are repeatable for all the specimens subjected to XCT inspection with the CrossFlow specimens demonstrating fiber preferential direction towards the x-axis.

5 Conclusions

In the present work, the mechanical behavior of injection molded polypropylene reinforced with glass fibers was investigated experimentally in a temperature range between −30 and 80 °C. The specimens, either oriented parallel to the injection molding direction or perpendicularly, appear to be highly affected by the temperature. Nevertheless, significant differences were noted between the InFlow and Cross-Flow specimens which are more evident in higher testing temperatures where the fibers are having a crucial role in the mechanical performance of such kind of materials. However, the fiber orientation is not the only key factor that affects the results since the corresponding content was found to be nonuniform. The typical failure mode of such kind of specimens was analyzed by means of X-ray computed tomography, observing 2 typical failures with different affected zones and characteristics.

In addition, from the analysis of the X-ray CT data, some crucial information was obtained regarding the fiber content and preferential direction. Regarding the fiber content, the specimens are composed from similar overall fiber volume fractions but locally there have been observed some serious deviations. This may lead to some considerations about the nonhomogeneity of the distribution of the reinforcement inside the material and the inhomogeneity of the material overall. Moreover, regarding the fiber orientation factors, significant observations were conducted regarding the preferential direction of the fibers through-the-thickness. In all the cases, the reinforcing agent of the polymer appears to have completely different directions in the midplane (core) part compared to the rest of the sample. Considering the above, the difference between the InFlow and CrossFlow specimens is attributed not only to the orientation of the specimens, and thus to the orientation of the fibers, but also to the inhomogeneity of the samples regarding their fiber volume fraction, both locally and globally.

Declarations

Conflict of interest The authors declare no competing interests.

References

1. Friedrich K, Almajid AA (2013) Manufacturing aspects of advanced polymer composites for automotive applications. App Compos Mater 20:107–128. https://doi.org/10.1007/s10443-012-9258-7
2. Patel M, Pardhi B, Chopara S, Pal M (2018) Lightweight composite materials for automotive-a review. Int Res J Eng Technol 5(11):41–47
3. Altenbach H, Altenbach J, Kissing W (2004) Mechanics of composite structural elements. Springer-Verlag, Berlin Heidelberg
4. Faroque R, Asjad M, Rizvi SJA (2021) A current state of art applied to injection moulding manufacturing process-a review. Mater Today Proc 43:441–446. https://doi.org/10.1016/j.matpr.2020.11.967
5. Morales G, Barrena MI, Gomez de Salazar JM, Merino C, Rodriguez D (2010) Conductive CNF-reinforced hybrid composites by injection moulding. Compos Struct 92:1416–1422. https://doi.org/10.1016/j.compstruct.2009.11.017
6. Jones RF (1998) Guide to short fiber reinforced plastics. Hanser Publishers, Munich
7. Papanathasiou TD, Guell DC (1997) Flow-induced alignment in composite materials. Woodhead Publishing Ltd
8. Jack DA, Smith DE (2007) The effect of fibre orientation closure approximations on mechanical property predictions. Compos Part A Applied Sc Manuf 38(3):975–82
9. De Monte M, Moosbuger E, Quaresimin M (2010) Influence of temperature and thickness on the off-axis behaviour of short glass fibre reinforced polyamide 6.6 - Quasi static loading. Compos Part A 41:859–871. https://doi.org/10.1016/j.compositesa.2010.02.018
10. Wang Z, Zhou Y, Mallick P (2002) Effects of temperature and strain rate on the tensile behaviour of short fiber reinforced polyamide 6. Polym Compos 23(5):858–871. https://doi.org/10.1002/pc.10484
11. Mortazavian S, Fatemi A (2016) Tensile behavior and modelling of short-fiber reinforced polymer composites including temperature and strain rate effects. J Thermoplast Compos Mater 30(10):1414–1437. https://doi.org/10.1177/0892705716632863
12. Mortazavian S, Fatemi A (2015) Effects of fiber orientation and anisotropy on tensile strength and elastic modulus of short fiber reinforced polymer composites. Compos Part B 72:116–129. https://doi.org/10.1016/j.compositesb.2014.11.041
13. Gupta M, Wang KK (1993) Fiber orientation and mechanical properties of short-fiber-reinforced injection-molded composites: simulated and experimental results. Polymer Composites 14(5):367–382. https://doi.org/10.1002/pc.750140503
14. Zainudin ES, Sapuan SM, Sulaiman S, Ahmad MMHM (2002) Fiber orientation of short fiber reinforced injection molded thermoplastic composites: a review. J Injection Molding Technol 6(1):1–10
15. Bay RS, Tucker CL (1992) Fiber orientation in simple injection moldings. Part II: experimental results. Polymer Composites 13(4):332–341. https://doi.org/10.1002/pc.750130410
16. Patcharaphun S, Mennig G (2007) Prediction of tensile strength for sandwich injection molded short-glass-fiber reinforced thermoplastics. J Met Mater Miner 17(2):9–16. https://doi.org/10.1002/PC.750100507
17. Miles IS, Rostami S (1992) Multi component polymer systems (polymer science and technology series). Longman Sci Tech Pub Group 1–435. https://doi.org/10.1002/pi.1994.210330319
18. Di Ilio A, Di Genova LG, Stamopoulos AG (2021) Implementation of the modified V-Notched Rail Shear method for characterizing glass fibre thermoplastic composites at sub-zero and elevated temperatures. Polym Test 93:106874. https://doi.org/10.1016/j.polymertesting.2020.106874
19. Benhadou M, Haddout A, Villoutreix G (2014) Numerical study of distribution and orientation of fibers during the injection of thermoplastic composites. J Reinf Plast Compos 33(18):1696–1703. https://doi.org/10.1177/0731684414543226
20. Miwa M, Horiba N (1993) Strain rate and temperature dependence of tensile strength for carbon/glass fibre hybrid composites. J Mater Sci 28:6741–6747. https://doi.org/10.1007/BF00356425
21. Li RKY, Lu SN, Choy CL (1995) Tensile and compressive deformation of a short-glass-fiber-reinforced liquid crystalline polymer. J Thermoplast Compos Mater 8(3):304–322. https://doi.org/10.1177/089270579500800306
22. Beaumont JP (2020) Running and gating design handbook. Tools for successful injection molding, 3rd edn. Carl Hanser Verlag Pub. https://doi.org/10.1016/C2014-0-02053-9
23. Rosato DV, Rosato DV, Rosato MG (2000) Injection molding handbook, 3rd edn. Kluwer Academic Publishers
24. ASTM D695-15 (2015) Standard test method for compressive properties of rigid plastics. Amer Soc Test Mater, PA
25. International Standard ISO 2818 (2018) Plastics-Preparation of test specimens by machining. Int Org Stan, ICS: 83-080-01-Plastics in general
26. Di Ilio A, Di Genova LG, Stamopoulos A (2021) Implementation of the modified V-Notched Rail Shear method for characterizing glass fibre thermoplastic composites in sub zero and elevated temperatures. Polymer Test 93:106874. https://doi.org/10.1016/j.polymertesting.2020.106874
27. Kumar SL, Aravind HB, Hossiney N (2019) Digital Image Correlation (DIC) technique in measuring strain in brick masonry specimen using Ncorr open source 2D MATLAB program. Res Eng 4:100061. https://doi.org/10.1016/j.rineng.2019.100061
28. Birt EA, Smith RA (2004) A review of the NDE methods for porosity measurement in fibre-reinforced polymer composites. Insight-Non-Destruct Test Cond Monit 46(11):681–686. https://doi.org/10.1784/insi.46.11.681.52280
29. Liu X, Chen F (2016) Defects characterization in CFRP using X-ray computed tomography. Polym Polym Compos 24(2):149–154. https://doi.org/10.1177/096739111602400210
30. Baran I, Straumit I, Shishkina O, Lomov S (2018) X-ray computed tomography characterization of manufacturing induced defects in a glass/polyester pultruded profile. Compos Struct 195:74–82. https://doi.org/10.1016/j.compstruct.2018.04.030
31. Stamopoulos AG, Tserpes KI, Prucha P, Vavrik D (2016) Evaluation of porosity effects on the mechanical properties of carbon fiber-reinforced plastic unidirectional laminates by X-ray computed tomography and mechanical testing. J Compos Mater 50(15):2087–2098. https://doi.org/10.1177/0021998315602049

32. Tserpes KI, Stamopoulos AG, Pantelakis SPG (2016) A numerical methodology for simulating the mechanical behavior of CFRP laminates containing pores using X-ray computed tomography data. Compos Part B 102:122–133. https://doi.org/10.1016/j.compositesb.2016.07.019

33. Chen H, Zhu W, Tang H, Yan W (2021) Oriented structure of short fiber reinforced polymer composites processed by selective laser sintering: the role of powder-spreading process. Int J Mach Tools Manuf 163:103703. https://doi.org/10.1016/j.ijmachtools.2021.103703

34. Hannesschläger C, Revol V, Plank B, Salaberger D, Kastner J (2015) Fibre structure characterisation of injection moulded short fibre-reinforced polymers by X-ray scatter dark field tomography. Case Stud Nondestruct Test Eval 3:34–41. https://doi.org/10.1016/j.csndt.2015.04.001

35. Baradi MB, Cruz C, Riedel T, Régnier G (2019) Mechanical and microstructural characterization of flowing weld lines in injection-molded short fiber-reinforced PBT. Polym Test 74:152–162. https://doi.org/10.1016/j.polymertesting.2018.12.017

36. Fiebig I, Schoeppner V (2016) Influence of the initial fiber orientation on the weld strength in welding of glass fiber reinforced thermoplastics. Int J Polym Sci 7651345:1–16. https://doi.org/10.1155/2016/7651345